Chapter 5

Neural network trained morphological processing for the detection of defects in fabric

5.1. Introduction

Traditionally, techniques of morphological image analysis have been used in many areas of interest mainly because of its simplicity and robustness [192]. In the area of textile inspection, the morphological processing algorithms have served to estimate non-woven features such as porosity, fiber orientation, and distribution [193]. Defect detection in fabric has been reported by using morphological operations [113, 194]. The binary morphological operations for the detection of defects were also tried and implemented in a laser-based system [54].

The morphological processing is usually done by passing a structuring element image on the binarized fabric image and then performing morphological operations, such as dilation, erosion, opening, and closing on the image. However, the main disadvantage of such morphological processing lies with the selection of structuring element. The size and shape of structuring element has to be different not only for different textures (i.e. class) of fabric but also for different types of defects to be identified.

In many applications of mathematical morphology, the structuring element remains invariant in shape and size as the image is probed and in general, the selections are done

heuristically or on trial and error basis. Several applications particularly in textural segmentation require the iterative application of successively larger structuring elements [195]. In order to overcome the problem, decomposition of the structuring element is proposed [196, 197]. One can also process (e.g. extract or eliminate) differently scaled objects of interest in the image by adapting the size of the structuring element(s) to the local intensity range [198]. Attempt has been made to use optimally selected structuring element [199] and optimal selection is applied for the defect detections in fabric [200].

Since biological neurons can adopt itself to a new situation and can be trained, it is necessary to evolve techniques of selection of structuring element by training from the image data to be processed for a specific application. In this chapter, a morphological processing technique is proposed for the detection of defects in fabric by training the system using an artificial neural network (ANN) model.

Artificial neural networks (ANNs) are used for defect detection due to their non-parametric nature and ability to describe complex decision regions [37]. The problem of fabric defect segmentation using feed-forward neural networks has been investigated earlier [201]. The back-propagation neural network [202] and neural network with the fuzzification technique have been used [203] to achieve the classification of different types of fabric defects. A framework for real time fabric defect detection using optical technique and neural network has also been evolved [72].

Though techniques of ANN have been applied for defect detection in fabric, it has not been tried as yet, in conjunction with the morphological operations where benefits of both the techniques can be exploited. The proposed technique involves in recording the test fabric image, converted into a de-noised gray scale image by morphological filtering operation with a small but fixed structuring element. After the noise removal, the interlaced warp and weft grating structure of the fabric is removed by correlating with a trained sliding widow structure. The resulting gray level image is then converted into binary image by thresholding

operation on the resultant data matrix. The intensity threshold level for binarization is also trained from ANN. Defects are then detected by morphological opening by reconstruction operation, for which a marker is required. The marker is nothing but another image obtained by morphological opening operation of mask image by suitable structuring element, whose size is also trained from an ANN. Multi-layer perceptron (MLP) model is used for training the network where optimized fabric parameters (i.e. features) are used instead of fabric images. In this chapter the optimized fabric features are represented in terms of optimized Haralick parameters as evolved in Chapter 4. The optimized Haralick parameters, representing the fabric classes are fed at the input layer of ANN along with the defect to be detected and the output of ANN gives dimensions of different structuring elements and threshold value required for morphological operations and binarization.

5.2 Morphological operations

The concepts and analytic tools of mathematical morphology for binary and gray images are derived from the set theory and integral geometry and can be performed both on binary and gray image with binary or gray structuring element [204, 205, 206]. In general, morphological operators transform an image into another image through the interaction with a structuring element image of certain shape and size [207, 208]. Depending upon the application geometric features of the images that are similar or dissimilar in shape and size to the structuring element are preserved, while other features are suppressed. Conventional symbols $\oplus$ and Θ denote morphological dilation and erosion operations, respectively.

5.2.1 Morphological operation on gray scale fabric images

Binary morphological operations, such as erosion, dilation, opening, and closing, are performed for the sets whose elements are vectors corresponding to pixel positions and

therefore are “set–set operations”. In most cases of defect detection, the algorithm is run on binary image of fabric. In contrast, a grayscale fabric image can be considered as a three-dimensional set, where the first two elements are *x* and *y* coordinates of a pixel and the third element is gray-scale intensity value. The key issue is to use the infima/ suprema (minima and maxima in discrete cases) to define grayscale morphological operators [209, 210]. The structuring elements of the gray-scale morphological operations can have the same domains as those in binary morphology. However, a gray scale structuring element is also possible having certain gray value instead of having only values “1” or “0” and can be decomposed [211]. Gray scale opening and closing are defined in a similar manner as in the binary case. The only difference when the operations are carried out, the opening and closing use gray scale dilation and erosion. As binary morphological operations do, gray scale opening is anti-extensive and gray scale closing is extensive.

Binary morphological operations are performed, in general, on binarized fabric image. Therefore, it is necessary to pre-process the fabric’s gray image to result in a binary image. To reduce the preprocessing steps, gray scale morphological operations on the gray scale fabric image are carried out in this case.

The structuring elements for the gray scale morphological operation can be of two types, namely, non-flat and flat. In non flat type structuring element the gray scale intensity values are not uniform everywhere and in the flat or binary type the pixels are bi valued 0 or 1. Normally the non- flat structuring elements are not used and operations with flat type are considered here.

5.2.1.1 Gray scale dilation

Let us consider that the p th gray scale fabric image of size $(M \times N)$ belonging to q th fabric class be denoted as, $f_p^q \in \Re^{(M \times N)}$, where $1 \le p \le P$ and $1 \le q \le Q$. Gray fabric

image is defined on a sub-section of two-dimensional Euclidean space $\Re^2 : \Re \cup \{-\infty, +\infty)$. In practice, however, the Euclidean space is replaced by a discrete space Z^2. The gray values taken by f_p^q are often limited to integers and are the pixel values at position (x, y). For 8-bit gray scale images, $f_p^q(x, y) : Z \rightarrow \{0,1,2....255\}$.

Let the flat structuring element of size $(m \times n)$ required for the gray scale morphological operation is denoted by $S_M \in \Re^{(m \times n)}$.

The dilation of f_p^q by a flat structuring element S_M at any location (x, y) is defined as the maximum value of the image in the window outlined by $\hat{S}_M$ within f_p^q, when the origin of $\hat{S}_M$ is at (x, y). Mathematically the operation is stated as,

$$[f_p^q \oplus S_M](x, y) = \max\{f_p^q(x - m', y - n') \mid (m', n') \in D_{S_M}\} \tag{5.1}$$

where, $\hat{S}_M = S_M(-x, -y)$ is the structuring element reflected about the origin and consists of the binary elements, D_{S_M} is the domain of S_M.

Thus the dilation operation with a flat structuring element, computes the maximum intensity values of f_p^q in the neighborhood. Figure 5.1 shows the dilation operation of the fabric image with a flat structuring element having varying size. As the size of structuring element increases the brighter portion in the fabric image also increases.

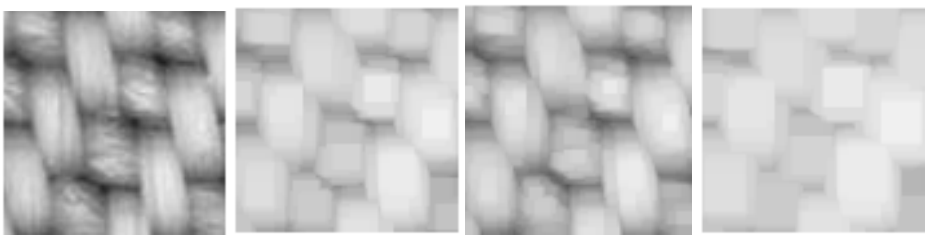

(a) *(b)* *(c)* *(d)*

Figure 5.1: (a) gray scale fabric image, (b)- (d) fabric images obtained by gray scale dilation of (a) by flat structuring elements of sizes (5×5), (10×10) *and* (15×15) *respectively.*

5.2.1.2. Gray scale erosion

The erosion of f_p^q by a flat structuring element S_M at any location (x, y) is defined as the minimum value of the image in the region coincident with S_M when the origin of S_M is at (x, y). The erosion operation is given by,

$$[f_p^q \Theta S_M](x, y) = \min\{f_p^q(x + m', y + n') \mid (m', n') \in D_{S_M}\} \tag{5.2}$$

where, D_{S_M} is the domain of S_M .

Thus the erosion operation with a flat structuring element, computes the minimum intensity values of f_p^q in the neighborhood. Figure 5.2 shows the erosion operation of the fabric image with a flat structuring element of varying size. As the size of the structuring element increases the darker part of the fabric image also increases.

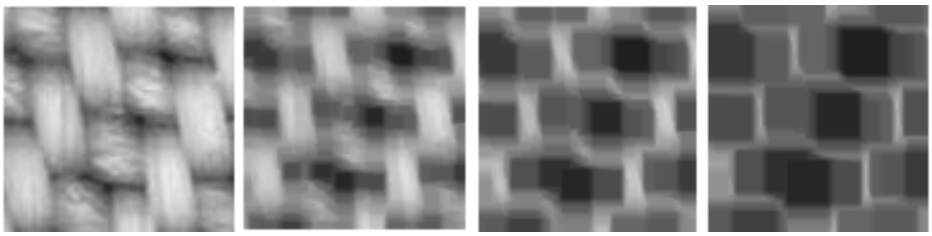

(a) *(b)* *(c)* *(d)*

Figure 5.2: (a) gray scale fabric image, (b)- (d) fabric images obtained by gray scale erosion of (a) by flat structuring elements of sizes (5×5), (10×10) *and* (15×15) *respectively.*

5.2.1.3. Gray scale opening

Opening of the gray scale image f_p^q by a flat structuring element S_M is defined as the erosion of f_p^q by S_M followed by a dilation of the result by S_M. The gray scale opening operation is represented as,

$$f_p^q \circ S_M = (f_p^q \Theta S_M) \oplus S_M \tag{5.3}$$

Thus by gray scale opening operation the intensity of all bright features of the fabric image are decreased, depending on the size of the structuring element. As the size of the structuring element increases the processed image becomes darker as shown in Figure 5.2.

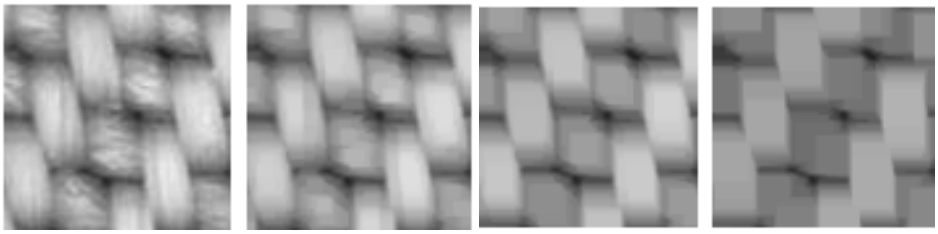

(a) *(b)* *(c)* *(d)*

Figure 5.3: (a) gray scale fabric image, (b)- (d) fabric images obtained by gray scale opening of (a) by flat structuring elements of sizes (5×5), (10×10) *and* (15×15) *respectively.*

5.2.1.4. Gray scale closing

Closing of the gray scale image f_p^q by a flat structuring element S_M is defined as the dilation of f_p^q by S_M followed by an erosion of the result by S_M. Mathematically the gray scale closing operation is represented as,

$$f_p^q \bullet S_M = (f_p^q \oplus S_M)\Theta S_M \tag{5.4}$$

Thus by gray scale closing operation the dark features of the fabric image are attenuated, depending on the size of the structuring element. As the size of the structuring element increases the fabric image becomes brighter. This is shown in Figure 5.4.

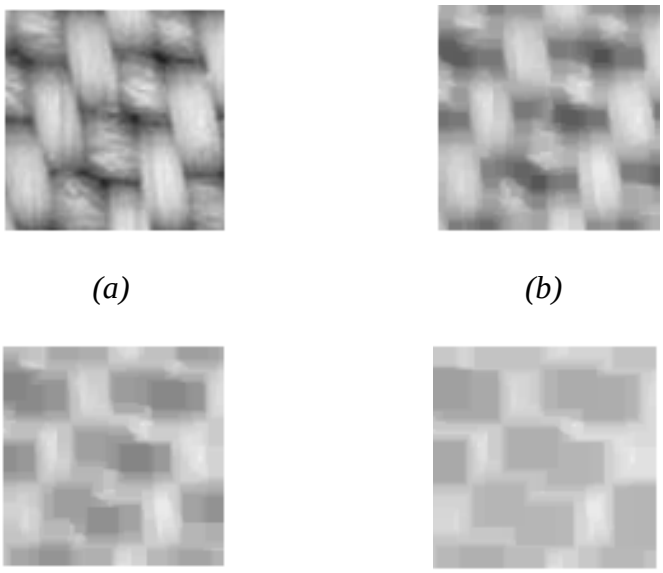

(a) *(b)*

(c) *(d)*

Figure- 5.4: (a) gray scale fabric image, (b)- (d) fabric images obtained by gray scale closing of (a) by flat structuring elements of sizes (5×5), (10×10) *and* (15×15) *respectively.*

In fact the gray scale opening operation suppresses brighter details smaller than the structuring element and gray scale closing operation suppresses the dark details smaller than the structuring element. These two techniques are often used in combination for the noise removal of the fabric image.

5.2.2. Gray scale opening and closing operations for de-noising the fabric image

Before applying the morphological operations for defect detection, the gray fabric image f_p^q is de-noised by using morphological filtering technique [212, 213]. This pre-processing is necessary particularly for defect detection in cotton fabric, where the presence of hairiness is more likely to occur and is reflected as noise in the fabric image. Since noise in an image should be removed wherever it is located, the property of translation invariance is required for any noise removing filtering. It is justifiable also for a fabric image where noise in the image is dimensionally smaller than the defects. The morphological filter, which can be

constructed on the basis of the underlying morphological operations, is more suitable for noise removal than the standard linear filters since the latter sometimes distort the geometric form of the image [214, 215]. The morphological filtering is restricted to all image–image transformations those are translation invariant, increasing, and idempotent operations.

Morphological representation of median filter is very useful for de-noising. The cascade of opening and closing with an elementary flat structuring element $S_M \in \Re^{(3\times3)}$ is used for this purpose. The de-noised fabric image f_p^{qD} is obtained from the gray scale fabric image by the gray scale closing operation of the gray scale fabric image followed by the gray scale opening operation, which mathematically is represented as,

$$f_p^{qD} \mid= [(f_p^q \bullet S_M) \circ S_M] \tag{5.5}$$

where, f_p^{qD} is the p th de-noised fabric belonging to q th fabric class.

Since the structuring element is symmetric, so reflection of S_M is S_M itself. By opening and closing operations, the noise present in the fabric image is removed while maintaining the shape and size of the defects almost intact.

Figures 5.5 (a) and (b) show a fabric image containing the 'salt & pepper' noise of various degree. The de-noised fabric image is given in Figure- 5.5 (c) and (d). In all the cases the flat structuring element of size (3×3) has been used.

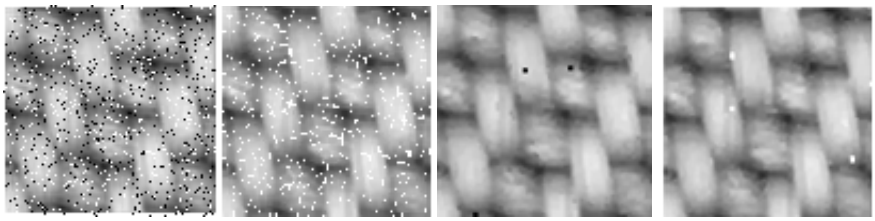

(a) (b) (c) (d)

Figure 5.5: (a) and (b) fabric image containing 'salt & pepper' noise, (c) and (d) are de-noised gray scale images.

5.3 Removal of interlaced grating structure due to warp and weft and binarization by thresholding

As already mentioned in previous chapters, during defect detection task, it is necessary to remove the grating structure of the fabric due to weft and warp interlacing without structurally altering the shape and size of the defects. To accentuate the gray scale values of the pixel positions of defects and to properly distinguish them from cross-points, it is also necessary to process the fabric image with a view to smooth out or remove the cross points. The processing is done by evaluating the correlation coefficients of the de-noised fabric image. For this purpose a sliding window of size $(a \times b)$ is translated over the entire fabric image of size $(M \times N)$. The correlation coefficient data matrix (CCDM) given by, $C_d \in \Re^{[M-(a-1))\times(N-(b-1)]}$ can now be formed from the de-noised fabric images f_p^{qD} by,

$$C_d(x,y) = \sum_y \sum_x f_p^{qD}[x:(x+a-1), y:(y+b-1)] \tag{5.6}$$

where, x and y vary from 1 to $[M-(a-1)]$ and 1 to $[N-(b-1)]$ respectively.

The de-noised fabric image f_p^{qD} is now converted into the binary image $F_p^{qD} \in \{0,1\}$ by selecting a proper threshold value θ_p^q of the corresponding correlation coefficient data matrix C_d.

5.4. Morphological opening by reconstruction operation for the detection of fabric defects

It is observed that in the de-noised binary fabric image, along with the image of the defect, some unconnected grains are present. These grains appear mainly due to incomplete removal of grating structure of the fabric and contain no information of defect(s). For the removal of these unconnected grains, the morphological opening operation by reconstruction is used.

This operation removes small objects, including some unconnected grains within defective portion and the subsequent dilation tends to restore the shape of the fabric defects which should remain intact. However maintaining the accuracy of this restoration is difficult as it depends on the similarity between the shapes of objects and structuring elements. Thus to extract the exact shape of fabric defect, while suppressing the grains, the morphological opening by iterative reconstruction operation is carried out.

The morphological opening by reconstructions extracts the connected components of de-noised binary fabric image F_p^{qD} called the *mask.* The mask is intersected by another binary image called *marker,* obtained by opening operation as,

$$F_p^{qM} = F_p^{qD} \circ S_{MC} \tag{5.7}$$

$S_{MC} \in \Re^{(u \times v)}$ is a flat structuring element of size $(u \times v)$, required for morphological opening operation.

To establish the dependence of marker on the morphological opening by reconstruction process a synthetic fabric image as shown in Figure 5.6(a) is considered. If a horizontal marker $S_{MC} \in \Re^{(1 \times v)}$ is taken for opening operation as given in equation 5.7, the opened image is shown in Figure 5.6(b) and the reconstructed image is shown in Figure 5.6(c).

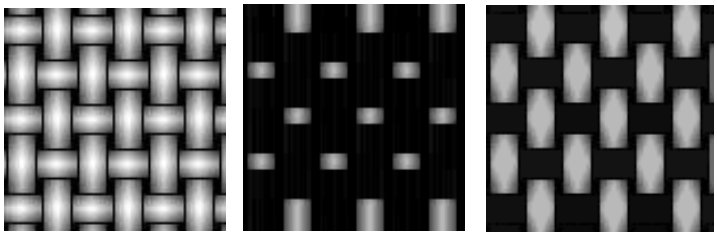

(a) (b) (c)

Figure- 5.6: (a) Synthetically generated fabric image taken as mask, (b) marker image, obtained by morphological open operation of (a) by a horizontal structuring element, (c) morphologically opened fabric image of (a) by reconstruction.

In the same way the results are shown in Figures 5.7(a), (b) and (c) while taking a vertical structuring element given by $S_{MC} \in \Re^{(u\times 1)}$ for morphological opening by reconstruction operation.

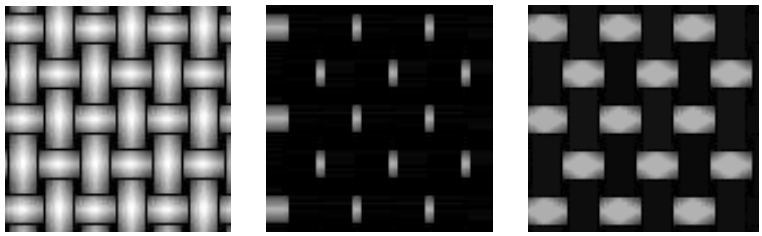

(a) (b) (c)

Figure- 5.7: (a) Synthetically generated fabric image taken as mask, (b) marker image, obtained by morphological open operation of (a) by a vertical structuring element, (c) morphologically opened fabric image of (a) by reconstruction.

Thus the dimension of $S_{MC} \in \Re^{(u\times v)}$ highly influences the process of defect detection by the morphological opening by reconstruction method, as it decides the nature of the marker.

The morphological reconstruction operation of the p th de-noised binary fabric image belonging to q th fabric class is obtained till the iteration shows no change in the resulting image. The process requires another structuring element $S^r \in \Re^{(3\times 3)}$ with all elements as 1 for getting 8 connectivity.

The image of defect $F_p^q|_{d_p}$ is now obtained as the result of a iterative process given by,

$$F_p^q|_{d_p}(t) = (\mathrm{F}_p^{qM} \oplus S^r) \cap F_p^{qD} \text{ till, } F_p^q|_{d_p}(t+1) = F_p^q|_{d_p}(t) \tag{5.8}$$

where, $F_p^q|_{d_p}(t)$ is the reconstructed p th fabric image of q th fabric class after t th iteration i.e. the image of the defect.

5.5 Selection of size of sliding window, structuring element for morphological open operation for getting marker and threshold value using ANN

There are three parameters which can be either heuristically controlled or can be trained by an ANN while performing morphological operations for the defect detection in fabric. The first parameter is the size of the sliding window $(a \times b)$ needed for the removal of the grating structure and for generating the correlation coefficient data matrix (CCDM). The second parameter is the threshold value θ_p^q, which converts the de-noised and grating removed gray scale fabric image into a binary fabric image. The third parameter is the size of the structuring element $(u \times v)$ for morphological open operation for getting marker, which is needed for the morphological open by reconstruction operation.

These three parameters, which are the output of ANN, need to be related with the fabric class for training ANN. For this purpose, each sample of fabric is assigned with a set of optimized Haralick parameters, (obtained in Chapter 4). During the training of ANN, corresponding to each training fabric image the set of optimized Haralick parameters of the fabric class, at which the training fabric image belongs, along with the nature of fabric defect to be detected act as set of input to ANN. The output parameters are the values of *a*, *b*, *u*, *v* and θ_p^q.

Once the ANN is trained properly these output parameters are obtained corresponding to the set of optimized Haralick parameters of the test fabric sample and the nature of fabric defect to be detected for the detection of defect.

To execute defect detection tasks, any simple ANN model may be useful for training [216, 217]. However, particularly in defect detection problems, where association of a single class is required for many disjoint regions in the pattern space, a multi layer perceptron

(MLP) model with a hidden layer of neurons is useful [218]. The hidden layer neurons generate hyper planes that are building blocks of decision regions. In MLP architecture, linear threshold unit is used for generating activation function from input layer neurons to the hidden layer neurons and sigmoidal threshold function is required for generating activation functions from hidden to output layer neurons. A real parameter λ determines the sigmoidal activation gain.

During the training process, up-gradation of the weight vectors takes place and continues till an error term ε goes below a certain pre-defined tolerance value. A learning rate coefficient η determines the size of the weight adjustments made at every iteration and hence influences the rate of convergence. Large learning rate may lead to oscillations during learning and it is necessary to introduce a momentum term α into weight update procedure. Many algorithms exist for training and testing in MLP model. Figure 5.8 shows the complete block diagram of the proposed processing steps used for the detection of defects in fabric of different fabric classes. The algorithm used for this purpose is given in Appendix- 5.1.

5.6. Test result on TILDA database

Optimum Haralick parameters obtained from the test fabric samples of a fabric class along with the nature of fabric defect to be detected are the inputs of the MLP architecture for defect detection. Once the training is complete, ANN gives the parameters a, b, u, v, θ_p^q as output required for the detection of the defects in the test fabric. The test fabric image is morphologically filtered for the removal of any noise that may be present in the test fabric. The resulting image is correlated over a sliding window of size $(a \times b)$ dictated by trained ANN. The intensity threshold value θ_p^q for the test fabric sample is also obtained from trained ANN. The resultant image is finally morphologically opened by reconstruction to get the defect that may be present in the test fabric sample. The marker required for the

morphological opening by reconstruction operation is obtained through the morphological open operation of the mask by a trained structuring element of size $(u \times v)$ dictated by ANN. The image thus obtained is binary and is then pixel-wise replaced so as to obtain the gray scale image of the defect.

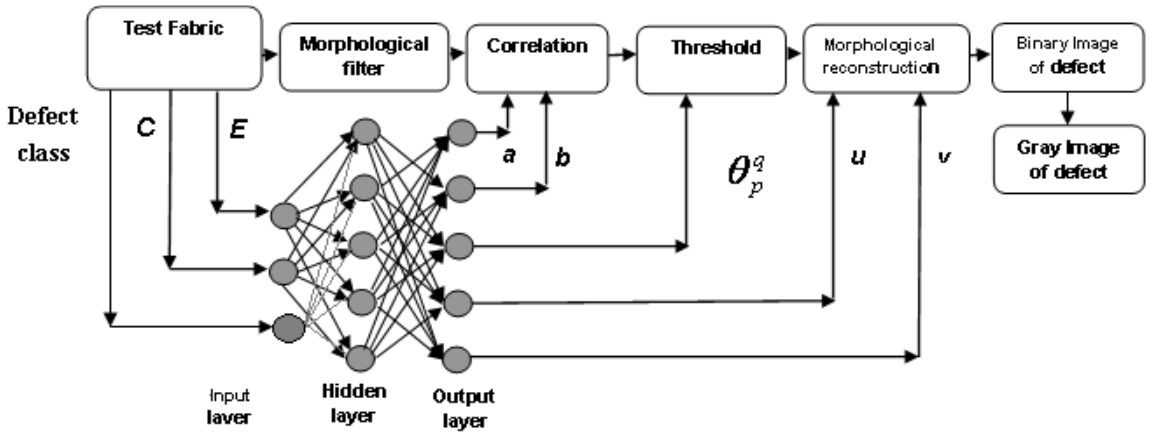

Figure 5.8: Block diagram of the process during test phase for the detection of defects in plain woven fabric.

Any type of fabric defects can be detected by training the system with the image of that defect. For testing the proposed method, TILDA [118] database for fabric defects is used. Images of TILDA database are 8-bit gray and of size (768 × 512) pixels. Three input neurons, five hidden neurons and five output neurons are used in MLP model of ANN. As for the given three fabric classes (fine, medium and coarse) only two Haralick parameters namely, energy (E), and correlation (C) are found to be the optimized Haralick parameters, so at the input layer three neurons corresponding to these two parameters and nature of defect to be detected are considered. As the trained ANN should output five parameters, namely, a, b, u, v, θ_p^q , so at the output layer five neurons are considered.

A total of 317 samples having eight types of defects in three types of woven fabrics are considered for testing purpose. The system is trained by at least ten and at most twenty

samples in each type of defect for each class of fabric. During testing 294 defective samples are correctly detected. Table 5.1 shows the test results.

Types of defects	Fine fabric		Medium fabric		Coarse fabric	
	Samples tested	Defects detected	Samples tested	Defects detected	Samples tested	Defects detected
Snarls/Loops/ Float thread	7	6	3	3	0	0
Small holes	17	14	19	17	9	9
Slub/ Fly	43	40	57	55	15	15
Thick yarn/ Reed mark	46	42	0	0	10	10
Thin places	4	3	2	2	0	0
Knots	7	7	5	5	3	3
Broken pick	0	0	10	9	23	22
Short pick	7	7	10	8	20	17
Total	131	119	106	99	80	76

Table-5.1: Test results for the detection of various defects.

Apparently the detection rate, as given by the ratio of the number of defective samples correctly detected to the total number of defective samples is calculated as 92.74% and the apparent detection success rate defined as the ratio of total number of samples correctly detected to the total number of samples is 92.5% when 83 more defect-free samples are also tested by the system making total number of samples tested as 400.

The false alarm rate, defined as the ratio of numbers of defect free samples detected as defective to the total numbers of defect free samples is 8.4%. Thus from the test result true positive (TP), false positive (FP), false negative (FN) and true negative (TN) values are estimated as 92.74%, 8.4%, 7.26% and 91.6% respectively. Thus the actual detection success rate given by the ratio of summation of TP and TN to the summation of TP, FP, FN and TN becomes 92.17%.

To give some illustrative examples, images for six test samples with different types of defects are shown in Figure 5.9. The first column shows six types of defects present in different types of fabrics. The third column indicates the images of fabric with interlaced grating structures removed.

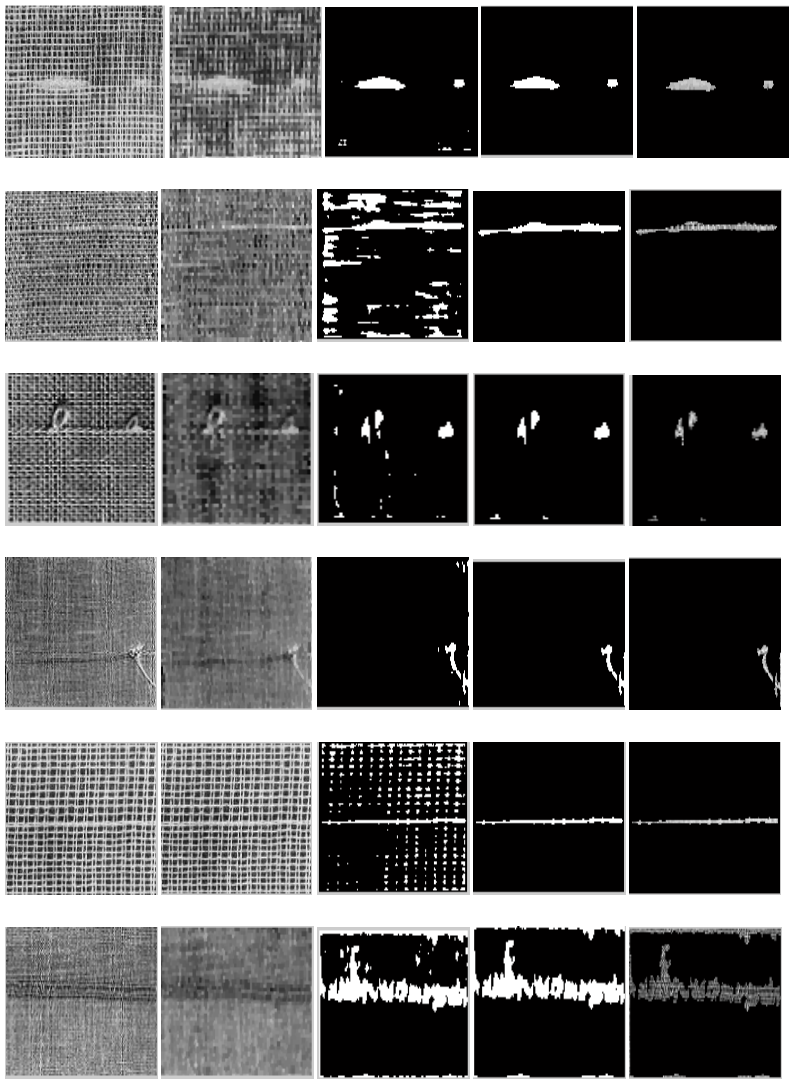

Figure 5.9: Test results of detection of various defects in the woven fabric (Column 1: fabric with various defects, Column 2: noise removed images after morphological filtering, Column 3: binary image after thresholding, Column 4: images after morphological reconstructions, Column 5: gray images of detected defects).

It may be seen that the interlaced structures are completely removed from fine fabric (fourth image from top of third column) whereas the structure is still visible in coarse fabric (fifth image from top of third column). Therefore, the present ANN needs to be trained from more data on coarse fabric. In fact the third column shows the binary images after thresholding.

It may be seen that small irregularities in weaving process and/or changes in illumination level are reflected in the images, which are particularly prominent in second image of third column, thus necessitating the reconstruction operations. The reconstructed images in the fourth column show the binary defects and those of fifth column show the gray scale images of the defects.

Moreover, if the test fabric contains multiple numbers of defects, the system is capable of detecting all of them as shown in Figure 5.10. However, if the types of defects on the same sample are different, then the system has to be trained separately for each type of defects for successful detection of each defect.

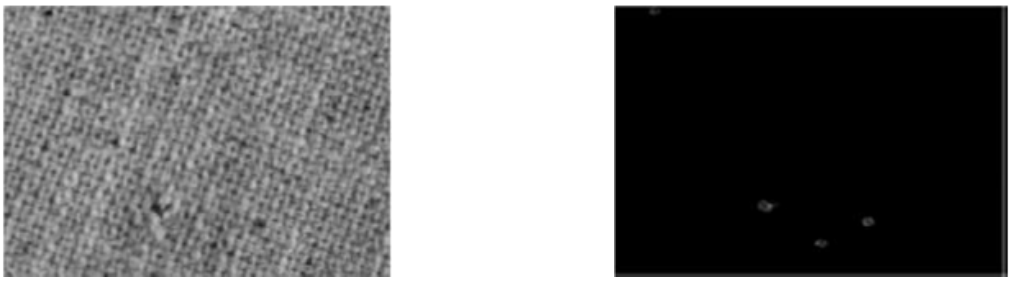

(a) *(b)*

Figure 5.10: Detection of multiple defects in a single test sample.

One interesting case of defect detection is presented in Figure 5.11, where the test fabric contains a thick yarn as defect. The fabric has an angular pattern of different yarn density than the basic interlacing of warp and weft. In stricter term, the angular pattern being regular

cannot be termed as defect. Therefore, the angular pattern is ignored by the proposed system while removing the interlaced structure. The defect is also detected correctly.

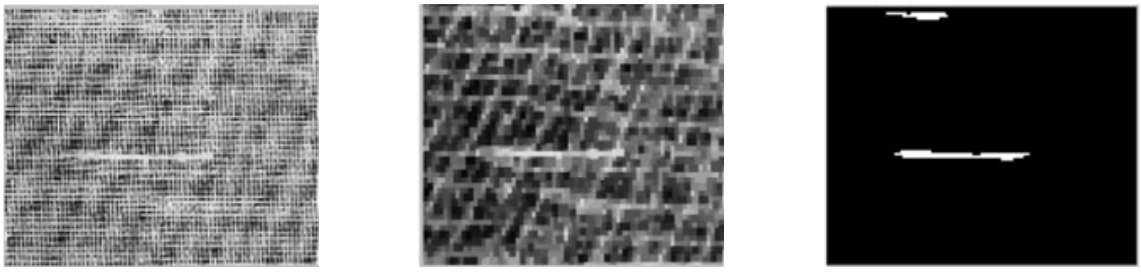

(a) (b) (c)

Figure 5.11: Typical case of defect detection with angular warp-weft structure: (a) fabric image, (b) morphological filtered image, and (c) image of defect.

5.7. Conclusions

From the results shown in Table 5.1, it can be concluded that training of the ANN and the MLP algorithm is satisfactory, as it gives almost the required values of the size of the windows, structuring element, and the threshold value for detection of different types of defects in different types of fabrics. It has been possible to train the system with images from a few samples and the detection rate of various types of defects is very good (92.8%). The image of the fabric is captured by a CCD camera assuming constant illumination. The major problems that occur are usually associated with the image of the fabric with non-uniform illumination since the variations in illumination generating sharp shades may be treated as defects by the system. Also it is necessary to consider how the technique can be applied in real time in a loom.

Appendix- 5.1 : Algorithm steps followed during the training of the ANN

1. Normalize the inputs and outputs with respect to the respective maximum values.
2. Select the number of neurons in the input, hidden, and the output layers as k, h and r, respectively, where in general, $1 < h < 2k$.
3. Select the values of λ (usually "1"), momentum coefficient α (usually positive and less than "1") and a tolerance value.
4. Initialize the weights connecting input layer neurons to hidden layer neurons, $[w_{ih}] \in \Re^{(h \times k)}$ and weights connecting hidden layer neurons to output layer neurons, $[w_{hO}] \in \Re^{(r \times h)}$, to some random normalized values lying between +1 and -1.
5. Apply one set of input vector $\{I\}_I \in \Re^{(k \times 1)}$ to the input layer. Assuming linear activation function, the output vector of the input layer is evaluated as $\{O\}_I = \{I\}_I$.
6. Compute the input vector $\{I\}_h \in \Re^{(h \times 1)}$ to the hidden layer as $\{I\}_h = [w_{ih}]\{O\}_I$
7. Calculate the hidden layer output vector $\{O\}_h \in \Re^{(h \times 1)}$ as,

$$\{O\}_h = [\frac{1}{(1+e^{-\{I\}_h})}]$$

8. Calculate the input vector of the output layer $\{I\}_O \in \Re^{(r \times 1)}$ as, $\{I\}_O = [w_{hO}]\{O\}_h$.
9. Calculate the output $\{O\}_O \in \Re^{(r \times 1)}$ of the output layer as,

$$\{O\}_O = [\frac{1}{(1+e^{-\{I\}_O})}]$$

10. Calculate the error vector $\varepsilon = [\varepsilon(1).....\varepsilon(e).....\varepsilon(r)]$

where, $\varepsilon(e) = [O_{Oe}|_{TARGET} - O_{Oe}]$; $O_{Oe}|_{TARGET}$ being the e th component of target output vector corresponding to the given input vector and O_{Oe} is the e th component of obtained output vector.

11. Find a vector $delta0 = [delta0(1).....delta0(e).....delta0(r)]$

where, $delta0(e) = \varepsilon(e).O_{Oe}.(1-O_{Oe})$ and $1 \le e \le r$.

12. Find another vector $deltawhO = \{O\}_h.delta0$.

13. The step of up-gradation of w_{hO} at $(t+1)$ th iteration becomes,

$$\Delta w_{hO}(t+1) = \alpha.\Delta w_{hO}(t) + \eta.deltawhO$$

14. Find a vector $delta1 = [delta1(1).....delta1(e).....delta1(h)] = [w_{hO}].delta0$

15. Find another vector $deltaH = [deltaH(1).....deltaH(e).....deltaH(h)]$

where $deltaH(e) = delta1(e).O_{he}.(1-O_{he})$ and O_{he} is the e th hidden neuron output.

16. Find one more vector as, $deltawih = \{O\}_I.deltaH$

17. The step of up-gradation of w_{ih} at $(t+1)$ th iteration becomes,

$$\Delta w_{ih}(t+1) = \alpha.\Delta w_{ih}(t) + \eta.deltawih$$

18 The mean square error of the entire data set is calculated repeating the steps from (5) to (17) for each iteration and the iterative process continues till the mean square error goes below a certain very low tolerance value, defined by the user